

**Ferromagnetic instabilities in neutron matter at finite temperature with the Skyrme interaction**

Arnau Rios and Artur Polls

*Departament d'Estructura i Constituents de la Matèria, Universitat de Barcelona, E-08028 Barcelona, Spain*

Isaac Vidaña

*Gesellschaft für Schwerionenforschung (GSI), Planckstrasse 1, D-64291 Darmstadt, Germany*

(Received 12 January 2005; published 19 May 2005)

The properties of spin-polarized neutron matter are studied at both zero and finite temperature using Skyrme-type interactions. It is shown that the critical density at which ferromagnetism takes place decreases with temperature. This unexpected behavior is associated to an anomalous behavior of the entropy that becomes larger for the polarized phase than for the unpolarized one above a certain critical density. This fact is a consequence of the dependence of the entropy on the effective mass of the neutrons with different third spin component. A new constraint on the parameters of the effective Skyrme force is derived if this behavior is to be avoided.

DOI: 10.1103/PhysRevC.71.055802

PACS number(s): 21.30.-x, 21.65.+f, 26.60.+c, 97.60.Jd

**I. INTRODUCTION**

Since the pioneering work of Vautherin and Brink [1] there has been an intensive use of Skyrme effective nucleon-nucleon ( $NN$ ) interactions to study properties of finite nuclei and nuclear matter, the latter mainly in conditions of astrophysical interest. This type of phenomenological  $NN$  interaction is thought to be used within a Hartree-Fock scheme (HF). Its zero-range character leads to simple analytical expressions for basic properties of symmetric nuclear matter such as the binding energy ( $a_b$ ), the saturation density ( $\rho_0$ ), the incompressibility modulus ( $K_\infty$ ), or the symmetry energy ( $a_s$ ). Actually, the experimental values of these quantities together with the binding energy of some doubly magic nuclei have been traditionally used to fit the parameters entering the general expression of a Skyrme force. The main advantage of these forces comes from their analytical character, which makes them very useful to get a physical insight into problems where the fully microscopic calculations are either very time consuming or not yet possible to implement. Once a parametrization is determined, one can, for instance, study nuclei and nuclear matter under conditions far from those used to fix the force in quite a simple way. In doing so, however, one must always keep in mind the particular limitations of the Skyrme parametrization that is being used.

By construction, most of the Skyrme forces used in the literature are well behaved around the saturation density of nuclear matter and for moderate isospin asymmetries. However, not all the Skyrme parameters are completely well determined through the fits of given sets of data and only certain combinations related to the basic properties mentioned above are really empirically determined [2]. This leads to a scenario where, for instance, different Skyrme forces produce similar equations of state for symmetric nuclear matter but very different results for neutron matter. This is easily understood if one considers that neutron matter or, equivalently, the systems with large isospin asymmetries are not part of the common input data that determine the parameters of the interaction. Obviously, this feature should be corrected if Skyrme-type forces are to be used in conditions of large neutron to proton

ratios such as nuclear matter inside neutron stars or nuclei near the drip line. Recently, several sets of Skyrme forces have been constructed taking into account different data coming from highly isospin asymmetric systems. The most well known among these are probably the parametrizations of the Lyon group (SLy interactions) [3,4], which also took into account variational results for neutron matter obtained with a realistic interaction [5] to fix the parameters of the force. Another important piece of input for neutron-rich systems are the isotope shifts of medium and heavy nuclei. In that case, modifications of the spin orbit term of the force have been taken into account to correctly reproduce the data. With these prescriptions, the SkI parametrizations were created almost a decade ago [6]. Recently, an extensive and systematic study has tested the capabilities of almost 90 existing Skyrme parametrizations to provide good neutron-star properties [7]. It was found that only twenty seven of these forces passed the restrictive tests imposed, the key property being the behavior (increasing) of the symmetry energy  $a_s$  with density.

Another situation of astrophysical interest refers to the possibility of the spontaneous appearance of spin polarized states in nuclear matter. This type of instability (i.e., a ferromagnetic transition at high densities) has long been studied using different theoretical methods [8–21]. The results are, nevertheless, still contradictory. On the one hand, Skyrme interactions predict several types of instabilities at increasing density [2]. In particular, currently used Skyrme forces show a ferromagnetic transition for neutron matter at densities in the range  $(1.1-3.5)\rho_0$  [22,23]. However, it has recently been shown that by including a small fraction of protons into the system, the onset density of ferromagnetism can be substantially reduced [24]. On the other hand, recent Monte Carlo simulations [25] and also Brueckner-Hartree-Fock calculations [26,27] using modern two- and three-body realistic interactions exclude such an instability, at least at densities up to 5 or 6 times  $\rho_0$ . This transition could have important consequences for the evolution of a protoneutron star, in particular for the spin correlations in the medium that do strongly affect the neutrino cross sections and the neutrino mean free paths inside the star [28].

Therefore, drastically different scenarios for the evolution of protoneutron stars are to be considered if the existence of such a ferromagnetic transition is confirmed.

Most of the studies of the ferromagnetic instability have been conducted at zero temperature. However, the description of protoneutron stars requires a study at finite temperature. Thus, because the general conditions for ferromagnetism are well established in the case of the Skyrme forces at zero temperature and even though their predictions are quite different than those of microscopic calculations, it is still interesting to study how the situation is modified at finite temperature. Intuitively, because of the thermal disorder, one would expect the onset density for ferromagnetism to increase with temperature. But, as shown later, the behavior turns out to be the opposite one and what actually happens is that the ferromagnetic transition takes place at smaller densities. In this work, we associate this fact to an anomalous behavior of the entropy as a function of the spin polarization. However, it is worth noticing here that there is no thermodynamical inconsistency in this dependence. If eventually, microscopic calculations with realistic interactions would not confirm this trend, we find out a new constraint on the parameters of the effective Skyrme force to avoid such a behavior.

In the next section we summarize the expressions of the energy and the single-particle energies at zero temperature and find the free energy and entropy at finite temperature for neutron matter as a function of the spin polarization. In Sec. III, we present some results involving the thermodynamical potentials of the system. Section IV is devoted to the study of the entropy, its relation to the effective mass and the possible constraints that could be imposed to the parameters to avoid such an anomalous behavior in both the classical and the low-temperature limit. Finally, the main conclusions are summarized in Sec. V.

## II. POLARIZED NEUTRON MATTER

Most of the Skyrme interactions used in the literature have the following general form:

$$\begin{aligned} V(\mathbf{r}_1, \mathbf{r}_2) = & t_0(1 + x_0 P^\sigma) \delta(\mathbf{r}) + \frac{1}{6} t_3(1 + x_3 P^\sigma) [\rho(\mathbf{R})]^\alpha \delta(\mathbf{r}) \\ & + \frac{1}{2} t_1(1 + x_1 P^\sigma) (\mathbf{k}'^2 \delta(\mathbf{r}) + \delta(\mathbf{r}) \mathbf{k}^2) \\ & + t_2(1 + x_2 P^\sigma) \mathbf{k}' \cdot \delta(\mathbf{r}) \mathbf{k} \\ & + i W_0(\sigma_1 + \sigma_2) [\mathbf{k}' \times \delta(\mathbf{r}) \mathbf{k}], \end{aligned} \quad (1)$$

with  $\mathbf{r} = \mathbf{r}_1 - \mathbf{r}_2$ ,  $\mathbf{R} = (\mathbf{r}_1 + \mathbf{r}_2)/2$ ,  $\mathbf{k} = (\nabla_1 - \nabla_2)/2i$  the relative momentum acting on the right and  $\mathbf{k}'$  its conjugate acting on the left.  $P^\sigma = (1 + \vec{\sigma}_1 \cdot \vec{\sigma}_2)/2$  is the spin exchange operator. The last term, proportional to  $W_0$ , corresponds to the zero-range spin-orbit term, which does not contribute in homogenous systems and thus will be ignored for the rest of the article.

Let us consider a homogeneous system of neutrons characterized by a total density  $\rho$ , which is the sum of the spin-up ( $\rho_\uparrow$ ) and spin-down ( $\rho_\downarrow$ ) densities. At zero temperature, the total energy will be a function of  $\rho_\uparrow$  and  $\rho_\downarrow$  or, alternatively, of the total density  $\rho$  and the spin polarization parameter  $\Delta$ , defined as  $\Delta = (\rho_\uparrow - \rho_\downarrow)/\rho$ .

The total energy of this system in the Hartree-Fock approximation is given by the sum of the kinetic energy associated to the Fermi gas of polarized neutron matter and the expectation value of the Skyrme interaction between the wave function describing two free Fermi seas corresponding to neutrons with two different spin orientations. These two Fermi seas have all the single-particle states characterized by a good linear momentum, occupied up to the Fermi levels  $k_{F\uparrow}$  and  $k_{F\downarrow}$  defined through  $k_{F\uparrow(\downarrow)} = (6\pi^2 \rho_{\uparrow(\downarrow)})^{1/3}$ .

The total energy per particle for zero temperature has the following expression:

$$\begin{aligned} e(\rho_\uparrow, \rho_\downarrow) = & \frac{\hbar^2}{2m} \frac{1}{\rho} [\tau_\uparrow + \tau_\downarrow] + \frac{1}{4\rho} [2t_2(1 + x_2)] [\tau_\uparrow \rho_\uparrow + \tau_\downarrow \rho_\downarrow] \\ & + \frac{1}{4\rho} [t_1(1 - x_1) + t_2(1 + x_2)] [\tau_\uparrow \rho_\downarrow + \tau_\downarrow \rho_\uparrow] \\ & + \frac{1}{\rho} [t_0(1 - x_0) + \frac{1}{6} t_3(1 - x_3) \rho^\alpha] \rho_\uparrow \rho_\downarrow. \end{aligned} \quad (2)$$

To simplify the notation, we will use from now on the symbol  $\sigma$  to indicate the third spin component. The functions  $\tau_\sigma$  are related to the average kinetic energy of the Fermi model of polarized neutron matter:

$$\tau_\sigma = \frac{3}{5} (6\pi^2 \rho_\sigma)^{2/3} \rho_\sigma = \frac{3}{10} (3\pi^2 \rho)^{2/3} \rho (1 \pm \Delta)^{5/3}, \quad (3)$$

where the plus (minus) sign corresponds to the up (down) spin projection. From the energy per particle one can easily derive the chemical potentials (up and down) and the pressure. Another important quantity for our analysis is the single-particle energy:

$$\epsilon_\sigma(k) = \frac{\hbar^2 k^2}{2m} + U_\sigma(k, \rho_\uparrow, \rho_\downarrow). \quad (4)$$

The single-particle potential  $U_\sigma(k, \rho_\uparrow, \rho_\downarrow)$  takes into account the interaction of a particle with momentum  $\mathbf{k}$  and spin projection  $\sigma$  with all the rest. It has a quadratic dependence on the momentum that is usually incorporated in the single-particle spectrum as a momentum independent effective mass:

$$\epsilon_\sigma(k) = \frac{\hbar^2 k^2}{2m_\sigma^*} + \bar{U}_\sigma(\rho_\uparrow, \rho_\downarrow), \quad (5)$$

where the effective mass is given by the following:

$$\frac{m_\sigma^*}{m} = \frac{1}{1 + \frac{2m}{\hbar^2} a_\sigma(\rho_\uparrow, \rho_\downarrow)}, \quad (6)$$

with

$$\begin{aligned} a_\sigma(\rho_\uparrow, \rho_\downarrow) = & \frac{1}{4} \{ [2t_2(1 + x_2)] \rho_\sigma \\ & + [t_1(1 - x_1) + t_2(1 + x_2)] \rho_{-\sigma} \}. \end{aligned} \quad (7)$$

The momentum independent part  $\bar{U}_\sigma$  of the single-particle potential  $U_\sigma$  is then written as follows:

$$\begin{aligned} \bar{U}_\sigma(\rho_\uparrow, \rho_\downarrow) = & \frac{1}{4} \{ [2t_2(1 + x_2)] \tau_\sigma \\ & + [t_1(1 - x_1) + t_2(1 + x_2)] \tau_{-\sigma} \} + [t_0(1 - x_0) \\ & + \frac{1}{6} t_3(1 - x_3) \rho^\alpha] \rho_{-\sigma} + \frac{1}{6} \alpha t_3 \rho^{\alpha-1} \rho_\sigma \rho_{-\sigma}. \end{aligned} \quad (8)$$

It is worth mentioning that the expression for  $\bar{U}_\sigma$  contains also the rearrangement term  $U_R(\rho_\uparrow, \rho_\downarrow)$ :

$$U_R(\rho_\uparrow, \rho_\downarrow) = \frac{1}{6}\alpha t_3 \rho^{\alpha-1} \rho_\sigma \rho_{-\sigma}, \quad (9)$$

which takes into account the effect of the density dependence of the effective interaction on the single-particle potential. Using this prescription for the single-particle potential, one can check that the chemical potential calculated from the energy per particle:

$$\mu_\sigma(\rho_\uparrow, \rho_\downarrow) = e(\rho_\uparrow, \rho_\downarrow) + \rho \left( \frac{\partial e(\rho_\uparrow, \rho_\downarrow)}{\partial \rho_\sigma} \right)_{\rho_{-\sigma}}, \quad (10)$$

does exactly coincide with the single-particle energies at the respective Fermi surfaces of each species,  $\mu_\sigma = \epsilon(k_{F\sigma})$ .

The extension of these expressions to finite temperature is rather straightforward. The expression for the internal energy and for the single-particle energy are exactly the same as in the zero temperature case, the only change coming from  $\tau_\sigma$ , which at finite temperature is given in terms of the so-called Fermi integrals [29]:

$$\tau_\sigma = \frac{g}{(2\pi)^2} \left( \frac{2m_\sigma^*}{\hbar^2} T \right)^{5/2} J_{3/2}(\eta_\sigma), \quad (11)$$

where  $g$  is the spin degeneracy factor of the system (in our case  $g = 1$  for each spin component) and where

$$J_\nu(\eta) = \int_0^\infty dx \frac{x^\nu}{1 + e^{x-\eta}}. \quad (12)$$

The parameter  $\eta_\sigma$  should be calculated by inverting the following equation:

$$\rho_\sigma = \frac{g}{(2\pi)^2} \left( \frac{2m_\sigma^*}{\hbar^2} T \right)^{3/2} J_{1/2}(\eta_\sigma), \quad (13)$$

which simply states, in terms of  $\eta_\sigma$ , that the integration of the Fermi momentum distribution of each spin component:

$$n_\sigma(k) = (1 + e^{\frac{\epsilon_\sigma(k) - \mu_\sigma}{T}})^{-1} \quad (14)$$

should coincide with the density of the component.

Once  $\eta_\sigma$  has been obtained, one can also calculate the chemical potentials at finite temperature:

$$\mu_\sigma(\rho_\uparrow, \rho_\downarrow, T) = \eta_\sigma T + \bar{U}_\sigma(\rho_\uparrow, \rho_\downarrow, T) \quad (15)$$

and the entropy per particle

$$s(\rho_\uparrow, \rho_\downarrow, T) = \frac{\rho_\uparrow}{\rho} s_\uparrow(\rho_\uparrow, \rho_\downarrow, T) + \frac{\rho_\downarrow}{\rho} s_\downarrow(\rho_\downarrow, \rho_\uparrow, T), \quad (16)$$

where the entropies of each component are given in the Hartree-Fock approximation by the following expression:

$$\begin{aligned} s_\sigma(\rho_\uparrow, \rho_\downarrow, T) &= -\frac{1}{\rho_\sigma} \int \frac{d^3k}{(2\pi)^3} \{n_\sigma(k) \ln n_\sigma(k) + [1 - n_\sigma(k)] \\ &\quad \times \ln[1 - n_\sigma(k)]\} \\ &= \frac{5}{3} \frac{1}{\rho_\sigma} \frac{1}{4\pi^2} \left( \frac{2m_\sigma^*}{\hbar^2} T \right)^{3/2} J_{3/2}(\eta_\sigma) - \eta_\sigma. \end{aligned} \quad (17)$$

Finally, for a fixed density and temperature, the suitable thermodynamical potential is the free energy. We can deduce

TABLE I. Symmetric nuclear matter properties at saturation density for SLy4 and SkI3. The corresponding value of the maximum mass of a neutron star obtained with the EoS of these two forces is also shown.

	$\rho_\infty$ (fm $^{-3}$ )	$a_v$ (MeV)	$a_s$ (MeV)	$K_\infty$ (MeV)	$M_{\max}$ ( $M_\odot$ )
SLy4	0.160	-15.97	32.04	230.9	2.04
SkI3	0.158	-15.98	34.89	259.2	2.19

it from the previous expressions of the energy and the entropy as follows:

$$f(\rho_\uparrow, \rho_\downarrow, T) = e(\rho_\uparrow, \rho_\downarrow, T) - T s(\rho_\uparrow, \rho_\downarrow, T). \quad (18)$$

From the free energy per particle, we can get the rest of the macroscopic properties of the system as, for instance, the pressure (and thus the EoS). In our case, we are particularly interested in the inverse magnetic susceptibility  $\chi^{-1}$ , which can be obtained from a second derivative of the free energy with respect to the spin polarization:

$$\frac{1}{\chi} = \frac{1}{\mu^2 \rho} \left( \frac{\partial^2 f}{\partial \Delta^2} \right)_{\Delta=0}, \quad (19)$$

where  $\mu$  is the magnetic moment of the neutron.

Notice that in our approach the effective mass  $m^*$  does not depend on the temperature and that the chemical potential obtained from the normalization condition of the density of each component (13), when the rearrangement is taken into account, coincides with the chemical potential derived from the free energy through its derivative with respect to density.

### III. ENERGETICS OF POLARIZED NEUTRON MATTER

For the discussion of our results we have chosen the SLy4 [4] and the SkI3 [6] Skyrme forces, both of which passed successfully the careful tests of Ref. [7]. In Table I, we report the values at saturation density of the binding energy, symmetry energy, incompressibility modulus, and maximum mass of the neutron star, which can be obtained using the EoS of these two Skyrme forces when the  $\beta$ -stability conditions in the presence of electrons and muons are imposed.

Because we are interested in analyzing the behavior of these forces with respect to the polarization of neutron matter, in Fig. 1 we report the ratio between the inverse magnetic susceptibility of interacting neutron matter and that of the corresponding free Fermi gas of neutrons as a function of the density for different temperatures. At zero temperature, as it is well known, both forces present a magnetic instability, that is, the previous ratio becomes zero at the critical densities ( $\rho_c = 0.60$  fm $^{-3}$  for SLy4,  $\rho_c = 0.37$  fm $^{-3}$  for SkI3), but, contrary to what can be intuitively expected, the onset density for the magnetic instability decreases with temperature for both forces. It is precisely this anomalous behavior that we want to explore here. Because we are mainly interested on the study of thermal effects, we have explored unrealistically high temperatures (much higher than those needed in the evolution of proto-neutron stars) in order to magnify them.

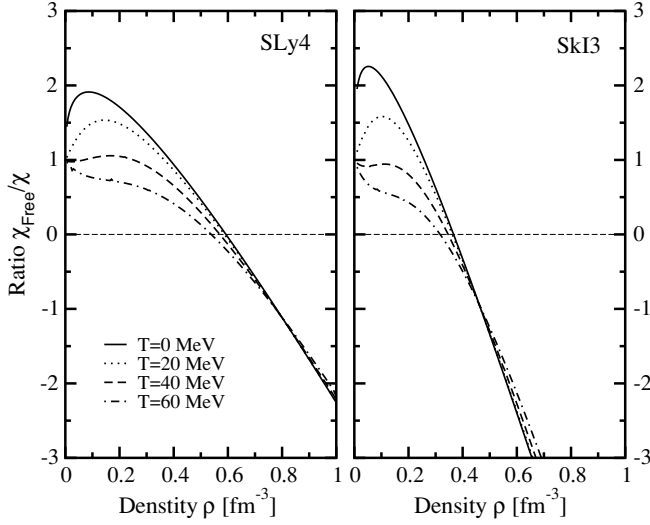


FIG. 1. Ratio between the magnetic susceptibility of the free Fermi gas and the corresponding magnetic susceptibility of interacting neutron matter as a function of density for several temperatures.

A complementary information that is rather helpful in this analysis is the difference between the free energy of totally polarized and unpolarized neutron matter. This difference as a function of density is reported in Fig. 2. Once this difference has become negative, the totally polarized system will have a lower free energy and therefore the system will prefer a polarized phase in front of the nonpolarized one. Notice that the density at which this difference becomes negative does not coincide with the onset of the magnetic instability. The critical densities defined by this criterium at zero temperature are  $\rho_c^F = 0.71 \text{ fm}^{-3}$  and  $\rho_c^F = 0.44 \text{ fm}^{-3}$  respectively, both of them larger than the corresponding  $\rho_{c.s}$ . The critical density  $\rho_c$  signals the density at which the unpolarized phase becomes unstable around  $\Delta = 0$ , which, however, does not imply that the system prefers the fully polarized phase, that is, the

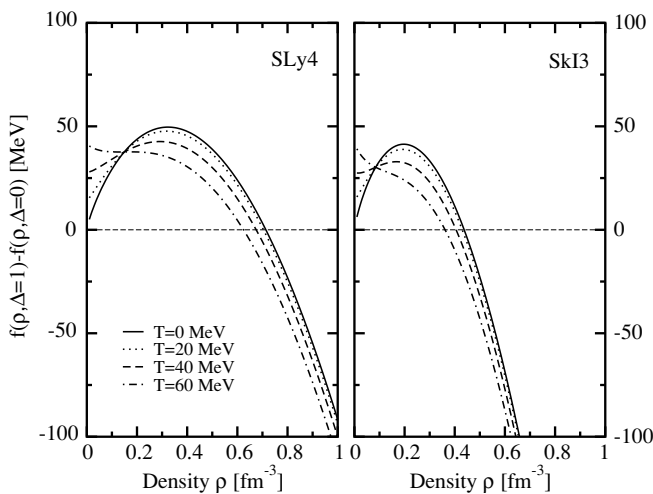


FIG. 2. Difference between the free energy per particle of fully polarized neutron matter and unpolarized neutron matter as a function of density for several temperatures.

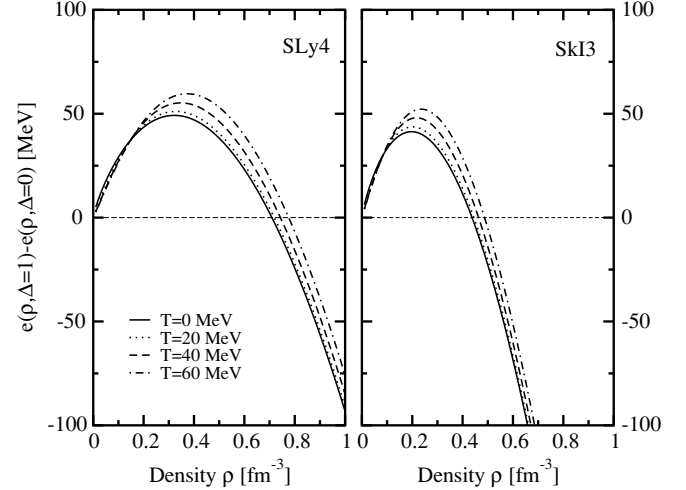


FIG. 3. Difference between the energy per particle of fully polarized neutron matter and unpolarized neutron matter as a function of density for several temperatures.

minimum of the free energy is not necessarily located at  $\Delta = 1$ . Even more, beyond  $\rho_c^F$ , as we will check later on, one cannot guarantee that the minimum of the free energy is located in the fully polarized system.

In this discussion, it is worth noticing that the energy per particle for fully polarized neutron matter with Skyrme interactions reduces to the following:

$$e(\rho, T, \Delta = 1) = \left[ \frac{\hbar^2}{2m} \frac{1}{\rho} + \frac{1}{2} t_2 (1 + x_2) \right] \tau_{\uparrow} = \frac{\hbar^2}{2m^*} \frac{1}{\rho} \tau_{\uparrow}, \quad (20)$$

where the effective mass  $m^*$  depends only on the parameters  $t_2$  and  $x_2$  as follows:

$$\frac{m^*(\rho, \Delta = 1)}{m} = \frac{1}{1 + \frac{2m}{\hbar^2} \frac{1}{2} t_2 (1 + x_2) \rho}. \quad (21)$$

This can be understood if one considers that the two body states of fully polarized neutron matter are all triplet states on both the spin and the isospin spaces, that is, they are symmetric in the spin-isospin variables, and, therefore, because of the Pauli principle, they do not see s-wave contributions (associated to the purely contact terms of the Skyrme force), but only  $p$ -waves originated from the gradient terms. As the parameter  $t_2$  is usually negative, one has to take  $x_2 \leq -1$  to avoid the collapse of fully polarized neutron matter [23]. Both SLy4 and SkI3 fulfill this condition. For SLy4, for instance,  $x_2 = -1$ . For this interaction, totally polarized neutron matter has  $m^*/m = 1$  and its energy reduces simply to the kinetic energy of a free Fermi sea.

The free energy is composed of the sum of two contributions, the internal energy and the entropy. Therefore, to understand the anomalous behaviour of the free energy, it is reasonable to analyze how both terms behave as a function of density. With this aim, we show in Fig. 3 the internal energy difference  $e(\rho, \Delta = 1, T) - e(\rho, \Delta = 0, T)$  as a function of the density for several temperatures. As expected, the density at which this difference becomes zero grows with temperature,

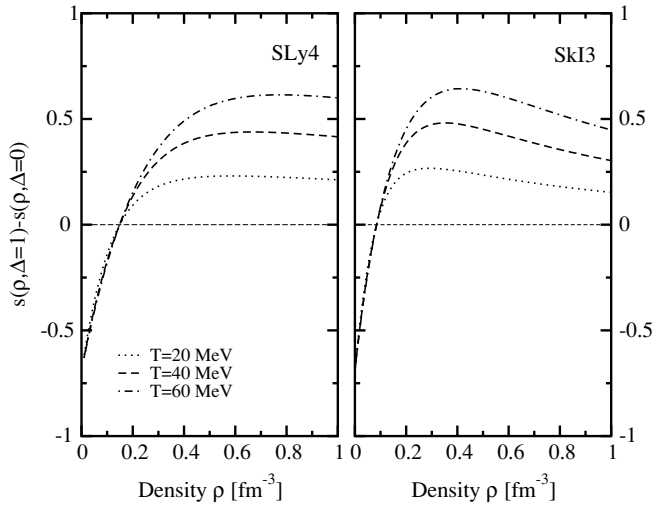


FIG. 4. Difference between the entropy per particle of fully polarized neutron matter and unpolarized neutron matter as a function of density for several temperatures.

so the origin of the surprising behavior detected in Fig. 2 should be attributed to the entropy contribution of the free energy.

The difference between the entropy of the polarized and the unpolarized phases is shown in Fig. 4 as a function of the density for three different temperatures. One would naively expect the entropy of the polarized system to be lower than that of the unpolarized one because, intuitively, the fully polarized phase is more “ordered” than the unpolarized one. This is, in fact, the behavior of the free Fermi sea. However, for the interacting system, the modification of the single particle properties, in particular those due to the effective mass, can invert this behavior even in the Hartree-Fock approximation. This inversion takes place at relatively low densities,  $\rho_c^S = 0.15 \text{ fm}^{-3}$  and  $\rho_c^S = 0.08 \text{ fm}^{-3}$  for SLy4 and SkI3 respectively, much smaller than the onset densities at which ferromagnetism appears. Notice also that the entropy critical densities are temperature independent.

As we have seen previously, there is a certain range of densities (between  $\rho_c$  and  $\rho_c^F$ ) where neutron matter is unstable around  $\Delta = 0$  but the fully polarized phase is still not energetically favorable. In this range (and also for densities a bit higher than  $\rho_c^F$ ), one can see that the minimum free energy happens at a partial polarization  $0 < \Delta < 1$ . This is seen in the left panel of Fig. 5, where we show the free energy of the system as a function of polarization at zero temperature (which of course coincides with the energy per particle) and for several densities, obtained with the SkI3 interaction. At densities below  $\rho_c$  (the critical density provided by the susceptibility criterium), the minimum energy takes place at  $\Delta = 0$  (this is the case of the first considered density,  $\rho = 0.32 \text{ fm}^{-3}$ ). When we overpass  $\rho_c$ , the minimum appears at an intermediate polarization and the energy of the fully polarized phase is still larger than the unpolarized one (this would be the case for  $\rho = 0.40 \text{ fm}^{-3}$ ). When the density increases, the minimum moves to larger values of  $\Delta$ , and, beyond  $\rho_c^F$ , we observe that  $f(\rho, \Delta = 0) > f(\rho, \Delta = 1)$  (this is the case for  $\rho = 0.48 \text{ fm}^{-3}$ ) even though the  $\Delta = 1$  phase is

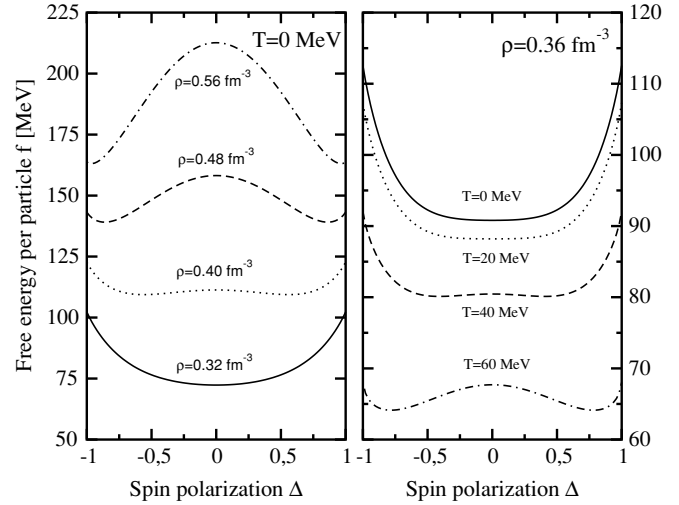


FIG. 5. (Left panel) Neutron matter free energy per particle at zero temperature as a function of polarization for several densities. (Right panel) Neutron matter free energy per particle at a fixed density  $\rho = 0.36 \text{ fm}^{-3}$  as a function of polarization for several temperatures. Both figures were obtained using the SkI3 force.

not the preferred one. Finally, for larger densities, the minimum shows up at the fully polarized configuration.

One can also observe the appearance of a preferred partial polarization as a function of the temperature for a given density, as it is illustrated in the right panel of Fig. 5 where the free energy per particle at  $\rho = 0.36 \text{ fm}^{-3}$  is drawn as a function of the polarization. At this density, the internal energy has the minimum at  $\Delta = 0$  for all the temperatures. However, the chosen density is above the onset density for the anomalous behavior of the entropy  $\rho > \rho_c^S$ , that is, the entropy is larger for the polarized phase. As a result, the free energy develops a minimum at  $0 < \Delta < 1$  that moves to higher polarizations when the temperature increases. Both panels of Fig. 5 are typical examples of a spontaneous symmetry breaking, where the interaction drives the ground state of the system to nonzero polarizations.

The spontaneous breaking of the spin rotational symmetry indicates the appearance of a phase transition in the system. In our case, this phase transition is between a nonpolarized and a polarized phase and the natural order parameter is, thus, the polarization. In Fig. 6 we report the polarization associated to the minimum of the free energy. For a given density and temperature, this is the polarization that gives the lowest free energy and it indicates, then, the polarization at which our system is thermodynamically stable. With this figure in hand, we can check all the results that we have been discussing up to now. At zero temperature, below  $\rho_c$ , the equilibrium configuration corresponds to  $\Delta = 0$ . Over  $\rho_c$ , the polarization grows steeply up to  $\Delta = 1$ . When the temperature increases, the curves shift to smaller densities, so  $\rho_c$  decreases with temperature and also the density at which the system becomes fully polarized. Of course, these results are somewhat academic because the densities needed for neutron matter to be fully polarized (in particular for SLy4) are very high and, thus, unattainable in a protoneutron star. However,

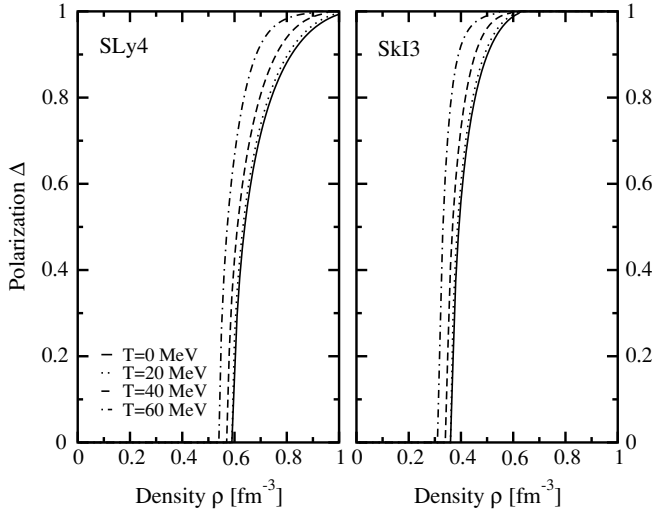


FIG. 6. Polarization associated to the minimum of the free energy for neutron matter as a function of density for several temperatures.

we find them useful because they serve to confirm the results concerning the anomalous behavior of the free energy with temperature.

#### IV. ENTROPY AND EFFECTIVE MASS

In this section we investigate the relation between the anomalous behavior of the entropy and the dependence of the effective mass on the polarization. To this end, we determine the density at which the difference between the entropy per particle of the fully polarized and the unpolarized phase becomes positive, that is, does not show the expected behavior  $s(\rho, T, \Delta = 1) - s(\rho, T, \Delta = 0) < 0$ . We explore two situations: the classical limit, defined by the condition  $\rho\lambda^3/g \rightarrow 0$  (with  $\lambda = \sqrt{2\pi\hbar^2/mT}$  being the de Broglie wavelength), and the degenerate limit, where  $T/\epsilon_F \ll 1$ .

In the first place, we consider the classical limit. In the interacting case, it is useful to introduce the de Broglie wavelength associated to the effective mass:

$$\lambda^* = \sqrt{\frac{2\pi\hbar^2}{m^*T}}. \quad (22)$$

It is worth reminding that, for Skyrme interactions, the effective mass depends on the density but is not affected by the temperature. In addition, it turns out that one can easily write all the relevant quantities for the nonpolarized system ( $\Delta = 0$ ) and the fully polarized one ( $\Delta = 1$ ). For instance, the internal energy can be casted in the following form:

$$e_{\text{cla}}(\rho, T, \Delta) = \frac{3}{2}T + U_1(\rho, \Delta), \quad (23)$$

where  $U_1(\rho, \Delta)$  is the contribution to the internal energy that cannot be included into the effective mass terms:

$$U_1(\rho, \Delta) = \frac{\rho}{4} \left[ t_0(1 - x_0) + \frac{1}{6}t_3(1 - x_3)\rho^\alpha \right] (1 - \Delta^2). \quad (24)$$

For the entropy, one has the following:

$$s_{\text{cla}}(\rho, T, g) = \frac{5}{2} - \ln \left[ \frac{\rho\lambda^{*3}}{g} \right], \quad (25)$$

where we have explicitly shown the dependence on the degeneracy factor  $g$ . To get the fully polarized case ( $\Delta = 1$ ), it is enough to set  $g = 1$ , whereas the nonpolarized case ( $\Delta = 0$ ) is obtained by setting  $g = 2$ . The previous expression can be splitted in two pieces, the entropy of a free gas plus a correction term associated to the effective mass:

$$s_{\text{cla}}(\rho, T, g) = \frac{5}{2} - \ln \left[ \frac{\rho\lambda}{g} \right] + \frac{3}{2} \ln \left[ \frac{m^*}{m} \right], \quad (26)$$

where one has to take into account that the effective mass depends on both the density  $\rho$  and the polarization  $\Delta$ . For the free case, one can in fact check that the expected inequality is fulfilled at all densities and temperatures:

$$s_{\text{cla}}(\rho, T, \Delta = 1) - s_{\text{cla}}(\rho, T, \Delta = 0) = -\ln 2 < 0. \quad (27)$$

In the interacting case, however, this difference becomes the following:

$$\begin{aligned} \Delta s_{\text{cla}}(\rho) &\equiv s_{\text{cla}}(\rho, T, \Delta = 1) - s_{\text{cla}}(\rho, T, \Delta = 0) \\ &= -\ln 2 + \frac{3}{2} \ln \left[ \frac{m^*(\rho, \Delta = 1)}{m^*(\rho, \Delta = 0)} \right], \end{aligned} \quad (28)$$

which clearly shows the influence of the interaction, via the effective mass, to the entropy difference and which turns out to be independent of the temperature. If we require the difference to be negative, the following condition should be satisfied:

$$\frac{m^*(\rho, \Delta = 1)}{m^*(\rho, \Delta = 0)} < 2^{2/3}. \quad (29)$$

Taking into account the expressions for the effective mass of the polarized and unpolarized phases for the Skyrme interactions [Eq. (6)], one gets the following condition for the parameters of the effective force:

$$\frac{1 + \frac{2m}{\hbar^2} \frac{\rho}{8} [t_1(1 - x_1) + 3t_2(1 + x_2)]}{1 + \frac{2m}{\hbar^2} \frac{\rho}{4} 2t_2(1 + x_2)} < 2^{2/3}. \quad (30)$$

The previous expression is not well defined whenever the denominator becomes zero. In fact, one can check that 11 of the 27 forces that passed the tests of [7] have a vanishing denominator at densities below  $0.5 \text{ fm}^{-3}$ . Because this denominator is nothing but the inverse effective mass for polarized neutron matter, such a singularity shows that these parametrizations were not devised to describe highly spin and isospin asymmetric matter. For the rest of the forces, one can check that  $m^*(\rho, \Delta = 1)/m^*(\rho, \Delta = 0)$  is a monotonically increasing function of the density, so we can univocally define a critical density  $\rho_c^{\text{cla}}$ . For SkI3, for instance, one can use Eq. (30) to obtain the critical density  $\rho_c^{\text{cla}} = 0.08 \text{ fm}^{-3}$ . The case for Skyrme Lyon forces is special, because most of them have  $x_2 = -1$  (the only exceptions are SLy0 and SLy2). In that simpler case, the previous condition reduces to the following:

$$1 + \frac{2m}{\hbar^2} \frac{\rho}{8} t_1(1 - x_1) < 2^{2/3}. \quad (31)$$

TABLE II. Densities  $\rho_c^S$  at which the condition (30) is violated for 16 different Skyrme forces. The respective critical densities  $\rho_c$  for the onset of ferromagnetism at  $T = 0$  are also shown.

	$\rho_c^S$ (fm $^{-3}$ )	$\rho_c$ (fm $^{-3}$ )
SGI	0.09	0.28
SLy0	0.11	0.41
SLy1	0.15	0.58
SLy10	0.13	0.61
SLy2	0.09	0.29
SLy230a	0.10	0.54
SLy3	0.15	0.60
<b>SLy4</b>	0.14	0.60
SLy5	0.15	0.57
SLy6	0.14	0.90
SLy7	0.14	0.57
SLy8	0.15	0.60
SLy9	0.11	0.47
SV	0.15	0.77
<b>SkI3</b>	0.08	0.37
SkI5	0.07	0.28

Then, as  $t_1(1 - x_1) > 0$ , one can easily obtain a critical density ( $\rho_c^{\text{cla}} = 0.15 \text{ fm}^{-3}$  for SLy4) beyond which one can be sure that, if the temperature is high enough to reach the classical limit, one will observe an anomalous behavior of the entropy. In fact, one can check that the temperature is not an essential factor because we have seen that  $\rho_c^S$  [precisely the density at which  $s(\rho, T, \Delta = 1) - s(\rho, T, \Delta = 0)$  changes sign] is quite independent of temperature and, thus, this classical entropy critical densities coincide with the  $\rho_c^S$  defined before,  $\rho_c^{\text{cla}} = \rho_c^S$ . In Table II we give a list of these densities for the 16 forces that have no singular effective mass for neutrons in fully polarized matter and compare it to the corresponding ferromagnetism onset densities at zero temperature  $\rho_c$ .

In second place, we investigate the low temperature limit. In this case, we can express the different thermodynamic quantities for the polarized and the unpolarized phases in terms of the Fermi momenta  $k_F = (6\pi^2\rho/g)^{1/3}$  and the Fermi energies associated to the effective mass  $\epsilon_F^*(\Delta) = \hbar^2 k_F^2 / 2m^*(\Delta)$ . In the low temperature regime, the internal energy can be written as (this expression is only valid for  $\Delta = 0$  or  $\Delta = 1$ ):

$$e_{\text{low}}(\rho, T, \Delta) = \frac{3}{5}\epsilon_F^*(\Delta) \left[ 1 + \frac{5\pi^2}{12} \left( \frac{T}{\epsilon_F^*(\Delta)} \right)^2 \right] + U_1(\rho, \Delta), \quad (32)$$

where  $U_1$  is the same function defined previously for the classical case and where we recover the well-known  $T^2$  dependence of the internal energy. Conversely, the entropy per particle (again only valid for  $\Delta = 0$  or  $\Delta = 1$ ) shows a linear dependence on  $T$ :

$$s_{\text{low}}(\rho, T, \Delta) = \frac{\pi^2}{2\epsilon_F^*(\Delta)} T = \frac{\pi^2}{3\rho} N(0)T, \quad (33)$$

where we have introduced the density of states at the Fermi surface,  $N(0) = gm^*k_F/2\pi^2\hbar^2$ .

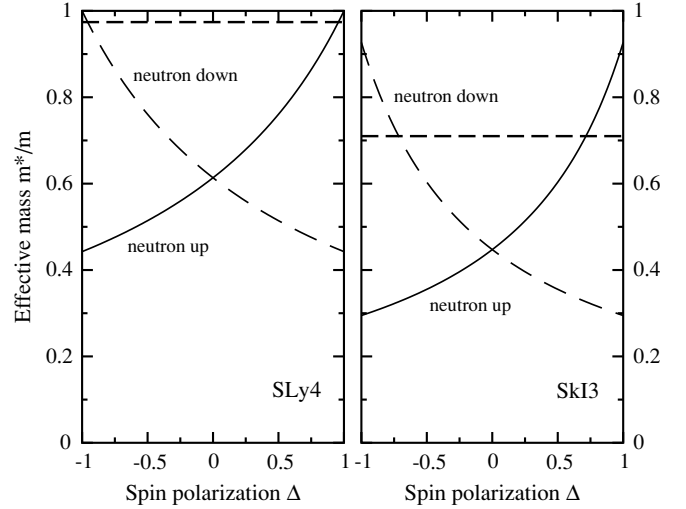


FIG. 7. Neutron effective mass of the up and down components as a function of polarization at  $\rho = 0.16 \text{ fm}^{-3}$ . The horizontal lines signal the maximum value of the effective mass of the up component in fully polarized matter if the entropy of the polarized phase has to be smaller than the unpolarized one.

At this point, we can perform the same analysis that we made for the classical limit. Let us start again by the free case and rewrite Eq. (33) to see the explicit dependence on the spin degeneracy:

$$s_{\text{low}}(\rho, T, \Delta = 1) - s_{\text{low}}(\rho, T, \Delta = 0) = \frac{\pi^2 T m}{\hbar^2 (6\pi^2 \rho)^{2/3}} (1 - 2^{2/3}), \quad (34)$$

which in fact is smaller than zero. For the interacting case, the difference comes, again, only from the effective masses:

$$\begin{aligned} \Delta s_{\text{low}}(\rho, T) &\equiv s_{\text{low}}(\rho, T, \Delta = 1) - s_{\text{low}}(\rho, T, \Delta = 0) \\ &= \frac{\pi^2 T m^*(\rho, \Delta = 0)}{\hbar^2 (6\pi^2 \rho)^{2/3}} \left[ \frac{m^*(\rho, \Delta = 1)}{m^*(\rho, \Delta = 0)} - 2^{2/3} \right]. \end{aligned} \quad (35)$$

By requiring this difference to be negative, we recover the same condition for the effective masses that we found in the classical regime [Eq. (30)]. Contrary to the classical limit, in this case  $\Delta s_{\text{low}}$  depends on the temperature, although this dependence cannot change its sign. Now we can understand why  $\rho_c^S$  is independent of the temperature: because in the classical limit (which requires high temperatures) and in the low temperature limit the entropy critical densities are exactly the same, one can guess that for intermediate temperature  $\rho_c^S$  will also not change.

We have seen that the interaction influences the entropy only through the effective mass and we have been able to trace back the anomalous behavior of the entropy (as a function of the polarization) to the violation of Eq. (30), which does involve only effective masses. In Fig. 7, then, we show the effective mass of neutrons with both orientations of the third spin component as a function of polarization for a fixed density  $\rho = 0.16 \text{ fm}^{-3}$ , which lies above the entropy critical density  $\rho_c^S$  for both SLy4 and SkI3. Obviously, for  $\Delta = 0$ ,

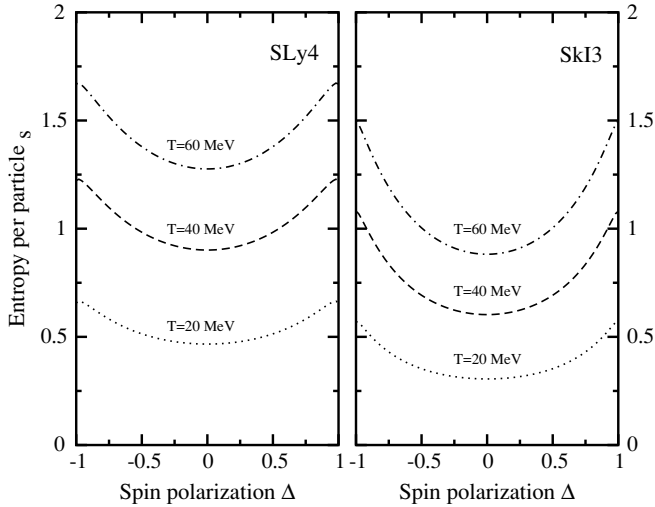


FIG. 8. Entropy per particle of neutron matter as a function of polarization at  $\rho = 0.32 \text{ fm}^{-3}$  for several temperatures.

the effective masses for the neutrons with spin up and spin down coincide. The horizontal line in both panels is placed at  $m^*/m = 2^{2/3}m^*(\Delta = 0)/m$ , indicating the upperbound for  $m^*(\Delta = 1)/m$ , above which we will find the anomalous behavior of the entropy. The effective mass of the most abundant species increases with the polarization, whereas the one of the less abundant is the decreasing one. Notice that for SLy4, as we have already pointed out, the effective mass for the fully polarized system is simply the bare mass.

The behavior of the entropy as a function of the polarization at a fixed density  $\rho = 0.32 \text{ fm}^{-3}$  for several temperatures and for both Skyrme forces is shown in Fig. 8. As expected, the entropy increases with temperature. However, because this density is above  $\rho_c^S$ , the entropy of the fully polarized phase is larger than that of the unpolarized one, giving the anomalous behavior of the entropy with the polarization. A careful look shows that this difference increases with temperature as expected from the results of Fig. 4. For a given temperature and polarization and considering that the entropy in both limits (and also in between them) is an increasing function of the effective mass and that, as shown in Fig. 7, the effective mass for SLy4 is larger than that of SkI3, we can understand why the entropy associated to SLy4 (left panel) is larger than the one corresponding to SkI3 (right panel).

Finally, using the low temperature expansion, we analyze why  $\rho_c^F$  decreases with temperature. At zero temperature, the difference between the free energy (internal energy) of the fully polarized phase and the nonpolarized one is follows:

$$\begin{aligned} \Delta f(\rho, T=0) &\equiv f(\rho, T=0, \Delta=1) - f(\rho, T=0, \Delta=0) \\ &= \frac{3}{5} \frac{\hbar^2}{2m^*(\rho, \Delta=1)} (3\pi^2\rho)^{2/3} \left[ 2^{2/3} - \frac{m^*(\rho, \Delta=1)}{m^*(\rho, \Delta=0)} \right] \\ &\quad - \frac{1}{4}\rho \left[ t_0(1-x_0) + \frac{1}{6}t_3(1-x_3)\rho^\alpha \right]. \end{aligned} \quad (36)$$

To find  $\rho_c^F(T=0)$ , we should find the density at which the previous expression becomes zero. For most of the forces, as we have already shown in Table II, the density at which

the first term becomes negative is quite low, whereas the combination  $[t_0(1-x_0) + \frac{1}{6}t_3(1-x_3)\rho^\alpha]$  is usually negative at all densities. The energy difference, then, becomes negative only through a balance of both terms, and this happens at  $\rho = \rho_c^F(T=0)$ , which is an upperbound for the real critical density  $\rho_c(T=0)$ . It is quite noticeable that this cancellation results from a subtle interplay of all parameters of the Skyrme force. Once we introduce a low temperature, the difference between free energies becomes the following:

$$\begin{aligned} &f(\rho, T, \Delta=1) - f(\rho, T, \Delta=0) \\ &= \Delta f(\rho, T=0) - \frac{\pi^2}{4} T^2 \frac{2m^*(\rho, \Delta=0)}{\hbar^2(6\pi^2\rho)^{2/3}} \\ &\quad \times \left[ \frac{m^*(\rho, \Delta=1)}{m^*(\rho, \Delta=0)} - 2^{2/3} \right], \end{aligned} \quad (37)$$

and, therefore, this relation shows that at finite temperature, whenever  $m^*(\rho, \Delta=1)/m^*(\rho, \Delta=0) > 2^{2/3}$ , which occurs for densities larger than  $\rho_c^S$ , the unpolarized system is unstable if the instability happens already at  $T=0$ . However, even when  $\Delta f(\rho, T=0) > 0$ , the second term can make the difference become negative. Around  $\rho_c^F(T=0)$ , the difference decreases with density (see Fig. 2) and thus the negative term makes  $\rho_c^F(T \neq 0)$  smaller with respect to  $\rho_c^F(T=0)$ . Or, in other words,  $\rho_c^F(T) < \rho_c^F(T=0)$  provided that  $\rho_c^F(T=0) > \rho_c^S$ , which is always true as seen in Table II.

## V. SUMMARY AND CONCLUSIONS

In this work, we have studied the properties of polarized neutron matter, with neutrons interacting through Skyrme-type interactions, both at zero and finite temperature. First, we have revised the zero temperature calculations using two modern Skyrme forces and we have studied the ground state of neutron matter as a function of polarization. We have shown that the ground state is not necessarily at fully polarized or unpolarized matter, but that it can be found at partially polarized matter, giving rise to a spontaneous symmetry breaking where the system prefers a state with nonzero polarization.

Our main emphasis, however, has been the study of the influence of temperature on the manifestation of the ferromagnetic behavior. In particular, we have considered the stability of the unpolarized phase and we have shown that the critical density at which ferromagnetism takes place  $\rho_c$  decreases with temperature. This unexpected behavior has been associated to an anomaly of the entropy: above a certain critical density  $\rho_c^S$ , the entropy of the polarized phase turns out to be larger than that of the unpolarized one. We have also shown that this fact is a consequence of the dependence of the entropy on the effective mass of the neutrons with different third spin component and, in particular, a consequence of the dependence of these effective masses on the polarization. More precisely, we have derived a condition for the maximum ratio between the effective masses of the fully polarized phase and the unpolarized one. Although this criterium is density dependent, one could in principle use it as a restriction on the parameters defining a Skyrme force.



Finally, we emphasize the fact that the present analysis has been restricted to Skyrme interactions that, contrary to other microscopic calculations, give a ferromagnetic transition at densities around  $3.5\rho_0$ . It would be useful to compare these calculations with the results obtained with realistic interactions and determine the behavior of the entropy and the effective masses of neutrons as a function of the spin polarization. Work in this direction is presently in progress.

#### ACKNOWLEDGMENTS

The authors are very grateful to Professors A. Ramos, J. Navarro, I. Bombaci, and J. Ortín for useful and stimulating discussions. This research was also partially supported by DGICYT (Spain) Project No. BFM2002-01868 and from Generalitat de Catalunya Project No. 2001SGR00064. One of the authors (A.R.) acknowledges the support from DURSI and the European Social Funds.

- 
- [1] D. Vautherin and D. M. Brink, *Phys. Rev. C* **3**, 626 (1972).
  - [2] J. Margueron, J. Navarro, and N. V. Giai, *Phys. Rev. C* **66**, 014303 (2002).
  - [3] E. Chabanat, P. Bonche, P. Haensel, J. Meyer, and R. Schaeffer, *Nucl. Phys.* **A627**, 710 (1997).
  - [4] E. Chabanat, P. Bonche, P. Haensel, J. Meyer, and R. Schaeffer, *Nucl. Phys.* **A635**, 231 (1998).
  - [5] R. B. Wiringa, V. Fiks, and A. Fabrocini, *Phys. Rev. C* **38**, 1010 (1988).
  - [6] P.-G. Reinhard and H. Flocard, *Nucl. Phys.* **A684**, 467 (1995).
  - [7] J. R. Stone, J. C. Miller, R. Koncewicz, P. D. Stevenson, and M. R. Strayer, *Phys. Rev. C* **68**, 034324 (2003).
  - [8] D. H. Brownell and J. Callaway, *Nuovo Cimento B* **60**, 169 (1969).
  - [9] M. J. Rice, *Phys. Lett.* **A29**, 637 (1969).
  - [10] J. W. Clark and N. C. Chao, *Lettere Nuovo Cimento* **2**, 185 (1969).
  - [11] J. W. Clark, *Phys. Rev. Lett.* **23**, 1463 (1969).
  - [12] S. D. Silverstein, *Phys. Rev. Lett.* **23**, 139 (1969).
  - [13] E. Østgaard, *Nucl. Phys.* **A154**, 202 (1970).
  - [14] J. M. Pearson and G. Saunier, *Phys. Rev. Lett.* **24**, 325 (1970).
  - [15] V. R. Pandharipande, V. K. Garde, and J. K. Srivastava, *Phys. Lett.* **B38**, 485 (1972).
  - [16] S. O. Bäckmann and C. G. Källman, *Phys. Lett.* **B43**, 263 (1973).
  - [17] P. Haensel, *Phys. Rev. C* **11**, 1822 (1975).
  - [18] A. D. Jackson, E. Krotscheck, D. E. Meltzer, and R. A. Smith, *Nucl. Phys.* **A386**, 125 (1982).
  - [19] S. Marcos, R. Niembro, M. L. Quelle, and J. Navarro, *Phys. Lett.* **B271**, 277 (1991).
  - [20] M. Kutschera and W. Wójcik, *Phys. Lett.* **B223**, 11 (1989).
  - [21] P. Bernardos, S. Marcos, R. Niembro, and M. L. Quelle, *Phys. Lett.* **B356**, 175 (1995).
  - [22] A. Vidaurre, J. Navarro, and J. Bernabeu, *Astron. Astrophys.* **135**, 361 (1984).
  - [23] M. Kutschera and W. Wójcik, *Phys. Lett.* **B325**, 271 (1994).
  - [24] A. A. Isayev and J. Yang, *Phys. Rev. C* **69**, 025801 (2004).
  - [25] S. Fantoni, A. Sarsa, and K. E. Schmidt, *Phys. Rev. Lett.* **87**, 181101 (2001).
  - [26] I. Vidaña, A. Polls, and A. Ramos, *Phys. Rev. C* **65**, 035804 (2002).
  - [27] I. Vidaña and I. Bombaci, *Phys. Rev. C* **66**, 045801 (2002).
  - [28] J. Navarro, E. S. Hernández, and D. Vautherin, *Phys. Rev. C* **60**, 045801 (1999).
  - [29] R. K. Pathria, *Statistical Mechanics*, Pergamon Press, New York, 1972.